Shortest Path in LEO Satellite Constellation Networks: An Explicit Analytic Approach

Quan Chen, Lei Yang, Yong Zhao, Yi Wang, Haibo Zhou, *Senior Member, IEEE*, and Xiaoqian Chen

***Abstract*— The Shortest Distance Path (SDP) problem is a critical routing issue in communication networks, particularly in satellite networks. Typically, SDP is solved by graph-based iterative algorithms, while an explicit or analytic approach is challenging. However, considering the orbit dynamics and topology regularity, this paper proposes, for the first time, an explicit analytic phase-based algorithm StepClimb to directly solve the SDP in low-Earth orbit (LEO) satellite networks. Based on the relationship between satellite phase and inter-satellite link distance, the SDP is modeled with the satellite phase, and SDP problem is converted into a total phase offset problem through theoretical derivations. Then StepClimb is derived in two cases, respectively. Monte-Carlo simulations verify StepClimb's accuracy, which has zero error in the mono-valley case and has less than 0.1% error in the bi-valley case. The algorithm performs better in larger-scale constellations and can save over 99.4% computational cost compared to Dijkstra algorithm. Further, the SDP pattern and features in Starlink constellation are analyzed. The model proves that most inter-plane hops in the SDP occur successively, and the simulations further indicate that these hops prefer satellites in the higher latitude regions.**

***Index Terms*— Shortest path, LEO satellite networks, routing, explicit analytic algorithm, mega-constellation network, starlink.**

I. Introduction

SHORTEST distance path (SDP) has been widely adopted in communication networks to achieve minimum network delay, optimal transmission cost, and maximum system efficiency [1], [2], [3], [4]. In LEO satellite networks connected by inter-satellite links (ISLs), SDP is also widely used to solve routing issues for low latency and high resource utilization [5], [6], [7].

The SDP solution is an extensively studied routing problem, and many classic SDP algorithms have been proposed and widely applied in practice, e.g., Dijkstra, Bellman-Ford [8], etc. Most of these algorithms are graph-based iterative algorithms that establish a graph and calculate the SDP through iterations over the graph. In LEO satellite networks, especially emerging mega-constellation networks [9], SDPs are also widely studied. Routing with a minimum distance or hop-count can greatly reduce the latency and network capacity usage.

Although conventional SDP algorithms are generic and applicable in various scenarios [10], [11], they are dependent on iterative computations and lack an intuitive explanation. All the link distances in the graph are required to be solved in a centralized manner. Also, the computational complexity increases greatly with the network scale, which may cause extra costs in mega-constellation networks [12], [13], e.g., Starlink, Kuiper, etc. This will result in large storage space requirements, long execution time of graph-based iterations and slow table lookup [14]. Therefore, an explicit and analytic algorithm to solve the SDP could provide more insights with fewer computations, and can be potentially integrated into a distributed routing protocol. However, deriving such an algorithm theoretically is challenging.

Different from other network systems, LEO satellite networks have unique topology features [15]. Although the topology is dynamic, the satellites are regularly placed in the constellations, their movements are ruled by deterministic orbit dynamics, and the inter-plane ISL distance varies with satellite phase, which provides opportunities for deriving an analytic approach. Chen et al. [16] exploit the topology features and propose an analytic model to calculate the required inter-satellite hops in mega-constellations. Some studies [17], [18], [19] have exploited the topology features of LEO constellations, but most still require iterative calculations to solve the SDP, and the explicit or analytic approaches are less studied.

Recently, preliminary propositions for theoretical analyses of SDP in LEO constellation networks have been derived [20]. The relationship between SDP and minimum hop path (MHP) and the judging criteria are strictly proved, and the results show that almost all SDPs are in the MHP set. Generally, SDPs are within the MHP set [21]. Then the SDP solution can be simplified and limited to the MHP region. Numerical studies [22], [23] further show that the path distance among the MHP set also has remarkable differences, mainly caused by the inter-plane ISL distance variation with the satellite phase. Therefore, using satellite phase to feature the path distance would be a promising way to derive an analytic solution.

Therefore, this paper aims to propose an explicit analytic approach to solve SDP, by exploiting the constellation topology regularity and link distance. Given a constellation and two satellites, the algorithm can directly output the exact SDP

Manuscript received 30 July 2023; revised 12 November 2023; accepted 19 December 2023. Date of publication 13 February 2024; date of current version 9 May 2024. This work was supported in part by the National Natural Science Foundation of China under Grant 11725211 and Grant 12002383 and in part by the Research Project of National University of Defense Technology under Grant ZK22-02. *(Corresponding authors: Quan Chen; Lei Yang.)*

Quan Chen, Lei Yang, and Yong Zhao are with the College of Aerospace Science and Engineering, National University of Defense Technology, Changsha 410073, China (e-mail: chenquan11@foxmail.com; craftyang@163.com; zhaoyong@nudt.edu.cn).

Yi Wang is with the Nanjing Research Institute of Electronics Technology, Nanjing 210013, China (e-mail: wangyi15@nudt.edu.cn).

Haibo Zhou is with the School of Electronic Science and Engineering, Nanjing University, Nanjing 210023, China (e-mail: haibozhou@nju.edu.cn).

Xiaoqian Chen is with the Chinese Academy of Military Science, Beijing 100091, China (e-mail: chenxiaoqian@nudt.edu.cn).

Color versions of one or more figures in this article are available at https://doi.org/10.1109/JSAC.2024.3365873.

Digital Object Identifier 10.1109/JSAC.2024.3365873

© 2024 The Authors. This work is licensed under a Creative Commons Attribution-NonCommercial-NoDerivatives 4.0 License.
For more information, see https://creativecommons.org/licenses/by-nc-nd/4.0/

shape, satellite nodes, and corresponding distance of the SDP. The algorithm has zero error when the satellite phases are close and has a minor error when satellite phases are far away. Since distance calculation of all the ISLs and graph-based iterations are avoided, the computational cost is also greatly reduced, especially in mega-constellation networks. The contributions are summarized as follows.

- Based on the LEO constellation topology and ISL distance features, the path distance is modeled by satellite phase, and the SDP problem is converted into a total phase offset problem through theoretical derivations.
- An explicit analytic phase-based algorithm StepClimb is derived in two cases based on the satellite positions. For the first time, given the constellation parameters, the SDP between any satellite pair can be directly calculated without graph-based iterations.
- Through Monte-Carlo simulations in various constellation scenarios, the proposed StepClimb is verified to be completely correct in mono-valley case and has less than 0.1% overall error if bi-valley cases is included. The algorithm performs even better in mega-constellations, reducing computational costs by over 99.4%.
- Simulations in Starlink scenario illustrate the SDP pattern variation with satellite movement. The model proves that most inter-plane hops in the SDP occur successively, and the simulations further indicate that these hops prefer satellites in the higher latitude regions.

The rest of this paper is organized as follows. The related studies and algorithms are discussed in Section II. Section III presents the LEO constellation network model and features of ISL distance, SDP, and MHP. Through derivations and proofs, Section IV proposes the novel StepClimb in two cases, respectively. The algorithm's applications, limitations, and advantages are also discussed. Then Section V verifies the proposed StepClimb through simulations in various constellation scenarios and further studies the SDP features in Starlink. Finally, Section VI concludes the whole paper.

II. Related Works

The SDP problem is a critical issue in satellite networks and has been widely studied. In LEO satellite networks, since the topology is time-varying, temporal graph-based models are adopted to generate several discrete snapshots, then the SDP is solved in each snapshot. Every node independently runs the graph-based algorithm to determine the SDP to every destination [14].

Pan et al. [17] leverage the terrestrial routing protocols OSPF and propose the Orbit Prediction Shortest Path First (OPSPF) algorithm for Resilient LEO Satellite Networks. Towards the random transmission requirements and stochastic packet generations/arrivals, Li et al. [18] portray the time-varying topology and propose an efficient Netgrid-based Shortest Path Routing (NSR) algorithm in large-scale satellite networks.

The Dijkstra algorithm is a generic and valid approach to obtain the optimal path in LEO satellite networks. Zhang et al. [14] run OSPF protocol which exploits Dijkstra to calculate the minimum hop-count between node pairs in integrated satellite and terrestrial Networks. In the hybrid multi-layered network [13], each MEO satellite uses Dijkstra algorithm to obtain the optimal routing table for each LEO satellite cluster. Dijkstra is also adopted to solve the favorable sequence of handovers in a graph-based user-satellite handover framework in LEO satellite networks [24]. Through the authors' literature research, most studies directly utilize classic algorithms to solve the SDP instead of developing new SDP algorithms in satellite networks. The existing solutions require iterations, while an explicit analytic SDP solution is not reported in satellite network field.

Since satellite topology is regular and predictable, the topological features are also exploited in path discovery. With four ISLs, the topology is mesh-like or torus-like, and the SDP can be approximately solved in the MHP region. A distributed LSP routing strategy [25] is proposed which selects the direction with more remaining hops in the MHP region. It can ensure a certain low latency while achieving congestion avoidance. Based on [16] and ISL distance features, Stock et al. [26] propose an approximate SDP algorithm DisCoRoute, which takes all the inter-plane ISL in the high-latitude regions where the inter-plane ISLs are shorter. The algorithm can achieve lower complexity, but it lacks theoretical derivation, and extra data e.g., satellite latitude and flying direction, are required. The concept of this algorithm is similar to the well-known DRA strategy [27].

In a more generic ISL topology, Chaudhry et al. [28], [29], [30] have exploited the topology features for inter-satellite paths with a more flexible ISL policy. The temporary links can enhance satellite connectivity and network connectivity, enabling better shortest paths between GSs in cities with lower propagation [28]. When the satellite connects farther neighbors, the network connectivity further improves with the increase in ISL range [29]. Moreover, the latency through laser ISL can be less than existing optical fiber terrestrial networks [30]. These results are novel and enlightening. However, considering current link capability and common practices, in this paper, we only focus on the typical four-ISL case.

III. System Model

A. LEO Constellation and Network Topology

A Walker-type constellation [31], [32] is adopted which involves regularly placing satellites at the same altitude h_s and inclination α. The placement can be denoted as $\alpha : N_P M_P / N_P / F$, where N_P orbit planes are distributed evenly along the equator, and M_P satellites are evenly distributed in each plane. The angle difference between the Right Ascension of Ascending Node (RAAN) of adjacent planes is $\Delta\Omega = 2\pi/N_P$ for Walker-delta type and $\Delta\Omega = \pi/N_P$ for Walker-star type, respectively. The satellite phase difference between adjacent satellites within the orbit plane is $\Delta\Phi = 2\pi/M_P$, and the satellite phase difference between satellites of adjacent orbits is $\Delta f = \frac{2\pi}{M_P N_P} F$, where F is the phasing factor and $F \in \{0, 1, \cdots, N_P - 1\}$.

The regular Walker-type constellation with a four-ISL pattern is the basic premise of this paper, which is widely

TABLE I

NOTATIONS AND DESCRIPTIONS

Notation	Description
α	Orbit inclination
$\Delta\Omega$	RAAN difference between adjacent orbits
$\Delta\Phi$	Phase between adjacent satellites within orbit
Δf	Phase difference between satellites in adjacent orbits
Δu	Phase between (1,1) and (M, N)
$d\,(P(M, N))$	Distance of $P(M, N)$
d^V, d^H	Distance of inter-plane and inter-plane ISL, respectively
F	Phasing factor
H	Minimum hops between two nodes
H^v, H^h	Minimum intra-plane and inter-plane hops, respectively
M, N	Dimension of the MHP region
M_P	Satellite number per plane
N_P	Orbit plane number
$P(M, N)$	Minimum-hop Path between satellite (1,1) and (M, N)
R	Number of successive inter-plane hops
u	Satellite phase
u_0	Phase of satellite (1,1)
$\widetilde{u}$	Phase offset between u and nearest U^s
U^s	Nearest axis of symmetry on u
$u(v_i)$	Satellite phase where the i-th inter-plane hop occurs
v_i	v-index of the i-th inter-plane hop
(v, h)	v-th satellite in h-th plane

adopted [10]. Satellite establishes four ISLs with their neighbors, two inter-plane ISLs and two intra-plane ISLs [33]. With the Pointing, Acquisition and Tracking (PAT) system [34], the ISLs can be maintained during the satellite movement. The ISLs form a mesh-like network topology, as shown in Fig. 1.

B. ISL Distance

In the same orbit plane, since the adjacent satellites have the same altitude and fixed phase difference, the intra-plane ISL distance keeps constant and can be given by

$$d^V = \sqrt{2}\,(R_E + h_s)\,\sqrt{1-\cos\Delta\Phi} \tag{1}$$

where R_E is the Earth radius and h_s is the orbit altitude. However, the inter-plane ISL distance varies with the instantaneous satellite phase u.

$$d^H = \sqrt{2}\,(R_E + h_s)\,\sqrt{1-\cos\Theta} \tag{2}$$

$$\begin{aligned}\cos\Theta = &\left(\cos^2(\Delta\Omega/2) - \cos^2\alpha\sin^2(\Delta\Omega/2)\right)\cos(\Delta f)\\ &- \cos\alpha\,\sin\Delta\Omega\,\sin\Delta f\\ &- \sin^2\alpha\sin^2(\Delta\Omega/2)\,\cos\,(2u+\Delta f)\end{aligned} \tag{3}$$

With the above equations, the distance of each ISL can be calculated. The inter-plane ISL distance is determined by orbit inclination α, inter-plane phase difference Δf, and RAAN difference $\Delta\Omega$, and varies with satellite phase u. The inter-plane ISL distance d^H varies with u, and the derivative can be calculated by

$$\frac{\mathrm{d}d^H}{\mathrm{d}u} = \frac{-\sqrt{2}\,(R_E+h_s)}{\sqrt{1-\cos\Theta}}\sin^2\alpha\sin^2(\Delta\Omega/2)\,\sin(2u+\Delta f) \tag{4}$$

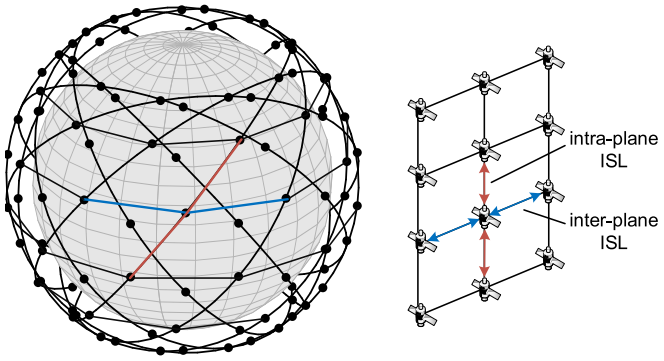

Fig. 1. LEO constellation and ISL network topology.

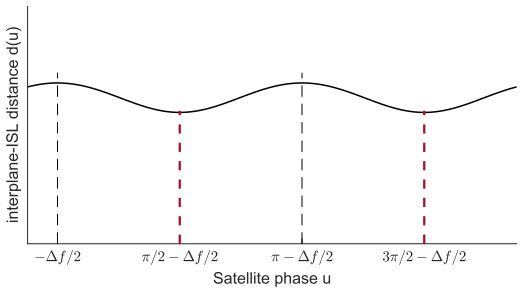

Fig. 2. The inter-plane ISL distance varies with the satellite phase.

The sign of $\frac{\mathrm{d}d^H}{\mathrm{d}u}$ can be determined by $\sin(2u+\Delta f)$. The inter-plane ISL distance increases with u from $k\pi-\frac{\pi}{2}-\frac{\Delta f}{2}$ to $k\pi-\frac{\Delta f}{2}$ and decreases with u from $k\pi-\frac{\Delta f}{2}$ to $k\pi+\frac{\pi}{2}-\frac{\Delta f}{2}$. Fig 2 gives the inter-plane ISL distance variation with the satellite phase. The distance has a variation period π and is symmetrical about $u=\frac{k}{2}\pi-\frac{\Delta f}{2}$.

C. MHP and SDP

With the four-ISL pattern, the satellite network forms a mesh-like topology that can be maintained although the ISL distances are varying. As shown in Fig. 3, given two satellite nodes A and B, packets of the minimum hop path from A to B have up to two alternative directions at each node. The minimum hops H between A and B is $H = H_v + H_h$, where H_v and H_h are the intra-plane and inter-plane hops, respectively. The MHPs between A and B can be not unique, but they have the same H, H_v and H_h, and form an MHP region. Due to the different satellite phases along the MHPs, the distances of the MHPs are also not identical.

The SDP is the path with minimum distance. Ref [20] has derived basic propositions with an explicit determinant function to judge if all the SDPs are in the MHP set. According to the results, all the SDPs are in the MHP set when the orbits are inclined or the phasing factors are larger. While in the rare exceptions in some near-polar constellations, only a few SDPs are not in the MHP set. In the following parts, we derive the SDP algorithm assuming that the potential SDP is within the MHP set, but the later analysis verifies that application of the algorithm is not limited to the premise.

D. Graph-Based SDP Solution

Many traditional SDP solutions have been widely applied in LEO constellation networks, e.g., Dijkstra and Bellman-Ford

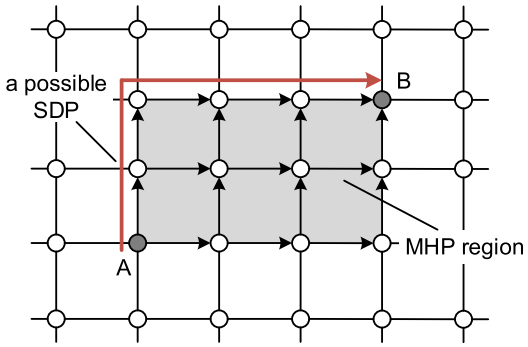

Fig. 3. SDP and MHP in constellation network topology.

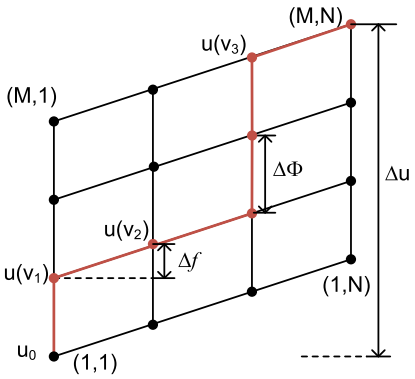

Fig. 4. The satellite phase where the inter-plane hops occur in a $M \times N$ MHP mesh (also a visual display for StepClimb pattern).

algorithms. In these algorithms, the network topology is modeled by a graph $G = (\mathcal{V}, \mathcal{E})$, where $\mathcal{V}$ is the set of all satellite nodes, and $\mathcal{E}$ is the set of all ISLs. All the topological connections are required and all the ISL distances need to be calculated as input. Then by iterative path relaxation through the whole graph, the SDP can be finally found.

According to the topology features of LEO constellations, if the SDP is specified within the MHP set, then the SDP search space can be simplified to a subgraph which can be regarded as a directed acyclic graph (DAG) [26]. By iterative path relaxation through the subgraph, i.e., the MHP region, the SDP can be found, and the computational complexity can be reduced. But the obtained SDP is not accurate in some special cases [20].

Different from the above graph-based iterative solution, this paper aims to derive a novel explicit analytic approach to directly solve the SDP, exploiting the constellation topology regularity and determinant ISL distance features.

IV. StepClimb for SDP Solution

In this section, first the SDP is specified by the positions where inter-plane hops occur, and path distance is explicitly modeled by the satellite phase. Then based on the phase difference between end satellite nodes, a novel algorithm StepClimb is derived in the mono-valley and bi-valley cases, respectively.

A. Formulations of Phase-Based SDP Distance

Given the source and destination satellite nodes, the MHP region forms a $M \times N$ dimension mesh-like region as shown in Fig. 4, where the source satellite and the destination node can be indexed as (1,1) and (M,N), respectively ($2 \le M \le \lfloor \frac{M_P}{2} \rfloor$, $2 \le N \le \lfloor \frac{N_P}{2} \rfloor$). (v, h) means the v-th satellite in the h-th plane in the MHP region. The satellite phase difference between two adjacent nodes is Δf for inter-plane ISL, while $\Delta\Phi$ for intra-plane ISL. Let the satellite phase of source node (1,1) $u_{1,1} = u_0$, then the phase of node (v, h) in the mesh is

$$u_{v,h} = u_0 + (v-1)\,\Delta\Phi + (h-1)\,\Delta f \tag{5}$$

Given a $M \times N$ dimension MHP, the intra-plane and inter-plane hops are $N-1$ and $M-1$, respectively. The distance of an MHP can be calculated by

$$d\left(P_{M,N}\right) = \sum\nolimits_{i=1}^{N-1} d_i^H + \sum\nolimits_{j=1}^{M-1} d_j^V \tag{6}$$

where d_i^H is the ISL distance of i-th inter-plane hop and d_j^V is the ISL distance of j-th intra-plane hop. Since d_j^V is fixed and the same for all intra-plane ISL and d_i^H varies at different satellites, (6) can be written as

$$d\left(P_{M,N}\right) = \sum\nolimits_{i=1}^{N-1} d_i^H + (M-1)\,d^V \tag{7}$$

The calculation of the SDP can be converted to finding the group of inter-plane ISLs with the total shortest distance which can form an MHP. More specifically, given a $M \times N$ dimension MHP region, we need to find the best positions for taking the $(N-1)$ inter-plane hops. The i-th inter-plane hop must occur at node $(*, i)$, then let v_i denote the v-index of the i-th inter-plane hop which occurs at node (v_i, i), $v_i \in \{1, 2, \ldots, M\}$, $i = 1, 2, \ldots, N-1$. Fig. 4 gives an example, where $v_1 = v_2 = 2$, and $v_3 = M$. Once $\{v_i\}$ is determined, the corresponding MHP is also determined. Then the problem is converted into finding the optimal set of v_i. Since the path pattern resembles 'Climbing Steps', the algorithm is named StepClimb, and the core idea is to find the optimal step locations, i.e., $\{v_i\}$.

In an MHP, $v_{i+1} - v_i$ means the number of intra-plane hops between the i-th and $(i+1)$-th inter-plane hops and we have $v_i \le v_{i+1}$. Let $u_{v_i,i}$ denote the phase of the satellite where the i-th inter-plane hop occurs, and hereafter $u_{v_i,i}$ is abbreviated as $u\left(v_i\right)$. According to Fig. 4, each intra-plane or inter-plane hop will cause a fixed phase change, then we have

$$u\left(v_i\right) = u_0 + \left(v_i - 1\right)\Delta\Phi + (i-1)\,\Delta f \tag{8}$$

where $i = 1, 2, \ldots, N-1$. Based on (8), we also have

$$u\left(v_{i+1}\right) - u\left(v_i\right) = \left(v_{i+1} - v_i\right)\Delta\Phi + \Delta f \tag{9a}$$

$$u\left(v_i\right) = u\left(v_1\right) + \left(v_i - v_1\right)\Delta\Phi + (i-1)\,\Delta f \tag{9b}$$

$$u\left(v_{i+1}\right) \ge u\left(v_i\right) + \Delta f \tag{9c}$$

$$u\left(v_1\right) = u_0 + \left(v_1 - 1\right)\Delta\Phi \tag{9d}$$

Then the problem of finding the SDP in the MHP set, i.e., $\min\limits_{d_i^H} d\left(P_{M,N}\right) = \min\limits_{d_i^H} \sum_{i=1}^{N-1} d_i^H + (M-1)\,d^V$, is equivalent to solving $\min\limits_{v_i} \sum_{i=1}^{N-1} d^H\left(u\left(v_i\right)\right)$.

Considering the symmetry and monotonicity of $d^H(u)$, $d^H(u)$ increases when u moves away from the axis of symmetry $u = U^s$, where $U^s = k\pi + \frac{\pi}{2} - \frac{\Delta f}{2}$. $\widetilde{u}$ is

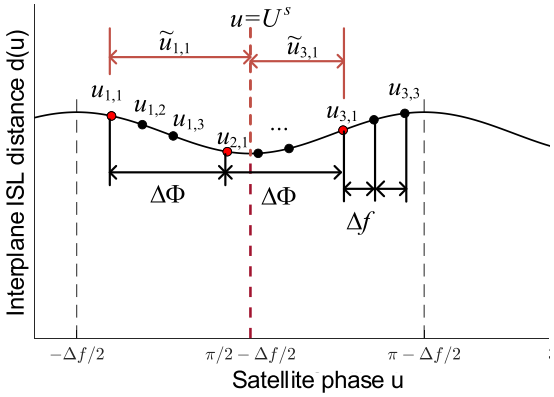

Fig. 5. Satellite phases and inter-plane ISL distances of the involved satellites in mono-valley case (between $-\frac{\Delta f}{2}$ and $\pi-\frac{\Delta f}{2}$).

defined as the phase offset between u and its nearest U^s, i.e., $|\widetilde{u}|=\min_k |u-U^s|$. $|\widetilde{u}|$ indicates the phase deviation from u to the min-distance position. Considering the period of $d^H(u)$ and U^s, $\widetilde{u}$ can be calculated by

$$\widetilde{u}=\mathrm{mod}\left(u+\frac{\Delta f}{2},\pi\right)-\frac{\pi}{2} \tag{10}$$

Then $\widetilde{u}(v_i)$ is the phase offset at the i-th inter-plane hop. Since d^H increases with $|\widetilde{u}(v_i)|$, we consider that the SDP has the minimum total path phase offset of all the inter-plane hop positions, which can be used to determine the SDP. The total path phase offset of all the inter-plane hop positions is denoted by

$$\widetilde{u}(P_{M,N})=\sum\nolimits_{i=1}^{N-1}|\widetilde{u}(v_i)| \tag{11}$$

Then the objective is to find $\{v_i\}$ to achieve $\min\sum_{i=1}^{N-1}|\widetilde{u}(v_i)|$. In the following derivations, the first step focuses on the path with minimum total phase offset, which is directly solved through theoretical derivations. Further, it is proved that the conclusions and solutions also apply to the SDP. Specifically, based on the relative phase positions of source and destination satellites, StepClimb is proposed in two cases, respectively.

B. Mono-Valley Case

The maximum phase difference of all the nodes in a $M\times N$ MHP region is calculated by

$$\Delta u=u_{M,N}-u_0=(M-1)\Delta\Phi+(N-1)\Delta f \tag{12}$$

When Δu is small, the source and destination satellites are relatively close. The phase of involved satellites may fall into the same 'valley' range as shown in Fig. 5 (between $-\frac{\Delta f}{2}$ and $\pi-\frac{\Delta f}{2}$), which is named the 'Mono-valley Case'. In this case, the closest axis of symmetry of all the nodes is the same one, which is denoted by $u=U^s$, $U^s=k_1\pi+\frac{\pi}{2}-\frac{\Delta f}{2}$. u_0 and Δu should satisfy $u_0,u_0+\Delta u\in\left[k_1\pi-\frac{\Delta f}{2},(k_1+1)\pi-\frac{\Delta f}{2}\right)$. Then $k_1=\left\lfloor\frac{u_0+\Delta f/2}{\pi}\right\rfloor$, and the mono-valley case specifies the exact range of Δu to $\Delta u\in\left[0,\frac{\pi}{2}-\widetilde{u_0}\right]$.

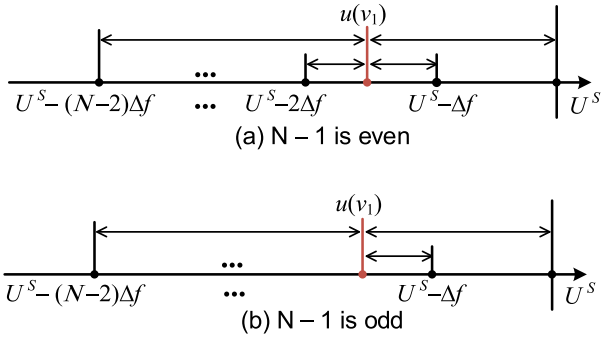

Fig. 6. Phase distance in the objective function (14) in mono-valley case.

Proposition 1: When $\Delta u\in\left[0,\frac{\pi}{2}-\widetilde{u_0}\right]$, *to achieve* $\min\widetilde{u}(P_{M,N})$, *the minimum hop path successively takes the inter-plane hops, i.e.,* $v_1=v_2=\ldots=v_{N-1}$.

The proof of Proposition 1 is provided in Appendix A. Proposition 1 indicates that in the mono-valley case, all the $(N-1)$-th inter-plane hops occur successively to minimize the total phase offset. Then $u(v_i)$ becomes

$$u(v_i)=u_0+(v_1-1)\Delta\Phi+(i-1)\Delta f \tag{13}$$

where $i=1,2,\ldots,N-1$. $\sum_{i=1}^{N-1}|\widetilde{u}(v_i)|$ is simplified to

$$\begin{aligned}\sum\nolimits_{i=1}^{N-1}|\widetilde{u}(v_i)|=&|u(v_1)-U^s|+|u(v_1)-(U^s-\Delta f)|\\&+\ldots+|u(v_1)-(U^s-(N-2)\Delta f)|\end{aligned} \tag{14}$$

Once the optimal v_1 is solved, the path with minimum total phase offset can be determined.

Proposition 2: When $\Delta u\in\left[0,\frac{\pi}{2}-\widetilde{u_0}\right]$, *to minimize* $\sum_{i=1}^{N-1}|\widetilde{u}(v_i)|$,

$$v_1=\arg\min_{v_1}\left|u(v_1)+\frac{N-2}{2}\Delta f-U^s\right| \tag{15}$$

The proof of Proposition 2 is provided in Appendix B. With Proposition 2, v_1 can be directly calculated. Since $u(v_1)=u_0+(v_1-1)\Delta\Phi$ and $u(v_1)-U^s=\mathrm{mod}\left(u(v_1)+\frac{\Delta f}{2},\pi\right)-\frac{\pi}{2}$, then $v_1=\arg\min_{v_1}\left|\mathrm{mod}\left(u_0+\frac{\Delta f}{2},\pi\right)+\frac{N-2}{2}\Delta f-\frac{\pi}{2}+(v_1-1)\Delta\Phi\right|$. Let the absolute value equal zero, we obtain an intermediate value

$$v_1^*=\frac{\frac{\pi}{2}-\mathrm{mod}\left(u_0+\frac{\Delta f}{2},\pi\right)-\frac{N-2}{2}\Delta f}{\Delta\Phi}+1 \tag{16}$$

Since $v_1\in\{1,2,\ldots,M\}$, finally v_1 can be calculated by

$$v_1=\max\{1,\min\{M,Round(v_1^*)\}\} \tag{17}$$

where $Round(x)$ denotes the standard rounding function that returns the integer closest to x. v_1 and (13) determine where the inter-plane hops occur, as well as the exact path. Next, we prove that the above condition and solutions are also applicable to achieve the shortest distance.

Proposition 3: When $\Delta u\in\left[0,\frac{\pi}{2}-\widetilde{u_0}\right]$, *to achieve* $\min_{v_i}\sum_{i=1}^{N-1}d^H(u(v_i))$, *the minimum hop path successively takes the inter-plane hops, i.e.,* $v_1=v_2=\ldots=v_{N-1}$.

The proof of Proposition 3 is provided in Appendix C. Proposition 3 indicates that in the SDP in the mono-valley case, all the inter-plane hops occur successively.

Proposition 4: When $\Delta u \in \left[0, \frac{\pi}{2} - \widetilde{u_0}\right]$, *if* $\sum_{i=1}^{N-1} |\widetilde{u}(v_i)|$ *is minimized,* $\min_{v_i} \sum_{i=1}^{N-1} d^H(u(v_i))$ *is also achieved, and* $v_1 = \arg\min_{v_1} \left|u(v_1) + \frac{N-2}{2}\Delta f - U^s\right|$.

The proof of Proposition 4 is provided in Appendix B. Proposition 4 indicates that in the mono-valley case when the total path phase offset is minimized, the path distance is also the shortest. Therefore, the conclusions of Proposition 1 and 2 are also the solution of the SDP. When the phases of end satellites satisfy the mono-valley case, first the v_1 can be directly calculated by (17), then the satellite where inter-plane hops occur can be determined by (13), and the shortest path distance can be also calculated. StepClimb for the SDP in the mono-valley case is summarized in Algorithm 1.

Algorithm 1 StepClimb for SDP in Mono-Valley Case

Input: Constellation parameters: N_P, M_P, α, h_s, F Info of source-destination satellites: M, N, u_0

Output: $\{v_i\}$, $d(P_{M,N})$

1: Calculate Δf, $\Delta\Omega$, $\Delta\Phi$;

2: $v_1^* = \frac{\frac{\pi}{2} - \mathrm{mod}\left(u_0 + \frac{\Delta f}{2}, \pi\right) - \frac{N-2}{2}\Delta f}{\Delta\Phi} + 1$, $v_1 = \max\{1, \min\{M, Round(v_1^*)\}\}$;

3: $v_i = v_1$, Calculate $u(v_i)$ according to (13);

4: Calculate d^V and d_i^H based on $u(v_i)$ and (1)-(3);

5: $d(P_{M,N}) = \sum_{i=1}^{N-1} d_i^H + (M-1)d^V$;

6: **return** $\{v_i\}$, $d(P_{M,N})$.

C. Bi-Valley Case

When Δu becomes larger, u_0 and $u_{M,N}$ can be in adjacent 'valleys', and the u range spans two valleys, which is named the 'Bi-valley Case'. The inter-plane hops may occur in either or both valleys. The above propositions are also suitable in each valley, but for the whole path, it is challenging to prove the applicability. Also, the calculation of the exact SDP becomes more complex in bi-valley case. Therefore, here we propose an approximate direct analytical solution using a similar framework as in the mono-valley case.

1) Problem Formulation: In the bi-valley case, u_0 and Δu should satisfy $u_0 \in \left[k_1\pi - \frac{\Delta f}{2}, (k_1+1)\pi - \frac{\Delta f}{2}\right)$ and $(u_0 + \Delta u) \in \left[(k_1+1)\pi - \frac{\Delta f}{2}, (k_1+2)\pi - \frac{\Delta f}{2}\right)$. The range of Δu can be specified to $\frac{\pi}{2} - \widetilde{u_0} \le \Delta u < \frac{3\pi}{2} - \widetilde{u_0}$.

Since in each valley, the above propositions in Section IV-B are also suitable, the inter-plane hops should be successively taken in each valley, then the SDP in bi-valley case can be simplified into a bi-step path where the inter-plane hops are successively taken in two segments, as shown in Fig. 7.

The bi-step path can be specified by three values: v_1, R, and Δv. From the source (1,1), the first inter-plane hop occurs at $(v_1, 1)$, and R inter-plane hops occur successively until $(v_1, R+1)$. After successive Δv intra-plane hops, the remaining $N-1-R$ inter-plane hops occur from $(v_1+\Delta v, R+1)$ to $(v_1+\Delta v, N)$, then the path reaches destination (M, N). To sum up, the $N-1$ inter-plane hops happen at

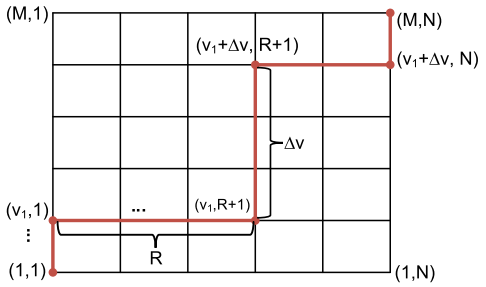

Fig. 7. A bi-step path in MHP region.

$$v_i = \begin{cases} v_1, & i = 1, 2, \ldots, R-1 \\ v_1 + \Delta v, & i = R, \ldots, N-1 \end{cases} \tag{18}$$

$$u(v_i) = \begin{cases} u_0 + (v_1 - 1)\Delta\Phi + (i-1)\Delta f, i = 1, 2, \ldots, R \\ u_0 + (v_1 + \Delta v - 1)\Delta\Phi + (i-1)\Delta f, i = R+1, \ldots, N-1 \end{cases} \tag{19}$$

Therefore, the SDP in the bi-valley case is uniquely specified by v_1, R, and Δv. The value ranges are $v_1 \in \{1, \ldots, M\}$, $R \in \{1, \ldots, N-1\}$, $\Delta v \in \{0, 1, \ldots, M-1\}$, and $v_1 + \Delta v \le M$.

Then we solve the optimal v_1, R, and Δv to minimize the total path phase offset $\widetilde{u}(P_{M,N}) = \sum_{i=1}^{N-1} |\widetilde{u}(v_i)|$ to obtain the shortest path. Let R satisfy $u(v_R) \le U^s + \frac{\pi}{2}$ and $u(v_{R+1}) \ge U^s + \frac{\pi}{2}$, then we have

$$|\widetilde{u}(v_i)| = \begin{cases} |u(v_1) + (i-1)\Delta f - U^s|, & i = 1, 2, \ldots, R \\ |u(v_1) + \Delta v\Delta\Phi + (i-1)\Delta f - U^s - \pi|, & i = R+1, \ldots, N-1 \end{cases} \tag{20}$$

Let $T_i = U^s - (i-1)\Delta f$, $i = 1, 2, \ldots, R$, and $T_j = U^s + \pi - \Delta v\Delta\Phi - (j-1)\Delta f$, $j = R+1, \ldots, N-1$, then the total path phase offset can be denoted by $\sum_{i=1}^{N-1} |\widetilde{u}(v_i)| = \sum_{i=1}^{R} |u(v_1) - T_i| + \sum_{j=R+1}^{N-1} |u(v_1) - T_j|$. The SDP problem in bi-valley case can be formulated as

$$\min_{v_1, R, \Delta v} \sum_{i=1}^{R} |u(v_1) - T_i| + \sum_{j=R+1}^{N-1} |u(v_1) - T_j| \tag{21a}$$

$$s.t. \quad u(v_1) = u_0 + (v_1 - 1)\Delta\Phi \tag{21b}$$

$$v_1 \in \{1, \ldots, M\}; \tag{21c}$$

$$R \in \{1, \ldots, N-1\}; \tag{21d}$$

$$\Delta v \in \{0, 1, \ldots, M-1\}; \tag{21e}$$

$$v_1 + \Delta v \le M \tag{21f}$$

2) An Approximate Direct Analytic Solution:

Since the undetermined values v_1, R, and Δv are interrelated, the calculation of (21) is complex. To simplify the calculation, we propose an approximate analytical solution using a similar framework as in mono-valley case.

The objective of (21) represents the sum of phase distances between $u(v_1)$ and T_i, T_j, as shown in Fig. 8. According to

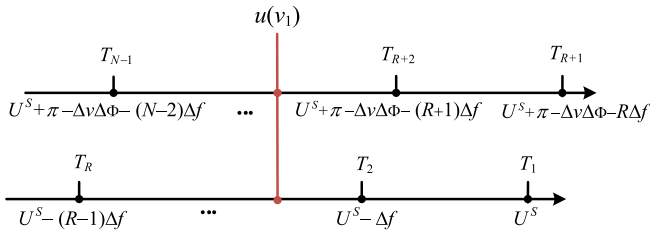

Fig. 8. Phase distance in the objective function in bi-valley case.

the objective function, to minimize the total phase distance, first we minimize the distance between two ends

$$\min_{R,\Delta v} \left|\max\left\{T_1, T_{R+1}\right\} - \min\left\{T_R, T_{N-1}\right\}\right| \tag{22}$$

where $T_1 = U^s$, $T_R = U^s - (R-1)\Delta f$, $T_{R+1} = U^s + \pi - \Delta v\Delta\Phi - R\Delta f$, and $T_{N-1} = U^s + \pi - \Delta v\Delta\Phi - (N-2)\Delta f$.

Eq (22) is a function of R and Δv, the results are that Δv should be closest to $\frac{\pi - \frac{N-1}{2}\Delta f}{\Delta\Phi}$, and R should be closest to $\frac{N-1}{2}$. Considering R should satisfy $u_0 + (R-1)\Delta f \le U^s + \frac{\pi}{2}$ and $u(v_i) - U^s = \widetilde{u}(v_i)$, we obtain an upper bound $R \le R_H$, where $R_H = \left\lfloor \frac{\frac{\pi}{2} - \widetilde{u_0}}{\Delta f} + 1 \right\rfloor$. R can be calculated by

$$R = \max\left\{1, \min\left\{R_H, round\left(\frac{N-1}{2}\right)\right\}\right\} \tag{23}$$

Then we calculate $\min_{v_1} \sum_{i=1}^{R} |u(v_1) - T_i| + \sum_{j=R+1}^{N-1} |u(v_1) - T_j|$. $u\left(v_1^H\right)$ should be closest to $\frac{1}{N-1}\sum_{i=1}^{N-1} T_i = \frac{1}{N-1}\left(\sum_{i=1}^{R} T_i + \sum_{i=R+1}^{N-1} T_i\right) = U^s + \frac{1}{N-1}\left(\frac{R(1-R)}{2}\Delta f + \frac{(N-1-R)(2\pi - 2\Delta v\Delta\Phi - (N-2+R)\Delta f)}{2}\right)$, then v_1 should be closest to $v_1^{**} = \frac{-\widetilde{u_0} + \frac{1-R}{2}\Delta f}{\Delta\Phi} + 1$.

Considering $u(v_R) \le U^s + \frac{\pi}{2}$, v_1 should also satisfy $v_1 \le v_H$, where $v_H = \left\lfloor \frac{\frac{\pi}{2} - \widetilde{u_0} - (R-1)\Delta f}{\Delta\Phi} \right\rfloor + 1$. Then we obtain v_1

$$v_1 = \max\left\{1, \min\left\{v_H, M, round\left(v_1^{**}\right)\right\}\right\} \tag{24}$$

Further, based on the results of (22), we can calculate Δv by

$$\Delta v = \max\left\{0, \min\left\{M - v_1, Round\left(\frac{\pi - \frac{N-1}{2}\Delta f}{\Delta\Phi}\right)\right\}\right\} \tag{25}$$

From (23)-(25), we can directly obtain the near-optimal solution of v_1, R, and Δv, respectively. Then the satellite phase of all the inter-plane hops can be calculated by (19), and the total distance of the approximate shortest path can be calculated by (1)-(3) and (7).

Note that in the bi-valley case, it is also possible that all the inter-plane hops are successively taken, which is an exceptional case, i.e., $\Delta v = 0$, $v_1 = v_2 = \ldots = v_{N-1}$, and $R = N - 1$. Then only v_1 needs to be determined, which can be solved using a similar method as the mono-valley case to minimize the $\sum_{i=1}^{N-1} |\widetilde{u}(v_i)|$. Finally, the optimal SDP is the path with the minimal $\sum_{i=1}^{N-1} |\widetilde{u}(v_i)|$. The approximate direct solution of the SDP in bi-valley case is summarized in Algorithm 2.

Algorithm 2 StepClimb for SDP in Bi-Valley Case

Input: Constellation parameters: N_P, M_P, α, h_s, F, Info of end satellites: M, N, u_0

Output: $\{v_i\}$, $d(P_{M,N})$

Calculate Δf, $\Delta\Omega$, $\Delta\Phi$;
$R = \max\left\{1, \min\left\{R_H, round\left(\frac{N-1}{2}\right)\right\}\right\}$, $v_1 = \max\left\{1, \min\left\{v_H, M, round\left(v_1^{**}\right)\right\}\right\}$, $\Delta v = \max\left\{0, \min\left\{M - v_1, round\left(\frac{\pi - \frac{N-1}{2}\Delta f}{\Delta\Phi}\right)\right\}\right\}$;
Calculate v_i and $u(v_i)$ according to (19);
$\widetilde{u}(P_{M,N}) = \sum_{i=1}^{N-1} |\widetilde{u}(v_i)|$;
Let $\Delta v = 0$ and $R = N-1$, calculate v'_1 and $\widetilde{u}'(P_{M,N})$;
if $\widetilde{u}(P_{M,N}) > \widetilde{u}'(P_{M,N})$ **then**
  $\Delta v = 0$, $R = N - 1$, and $v_1 = v'_1$;
  Update v_i and $u(v_i)$;
end if
Calculate d^V and d_i^H based on $u(v_i)$ and (1)-(3);
$d(P_{M,N}) = \sum_{i=1}^{N-1} d_i^H + (M-1)\, d^V$;
return $\{v_i\}$, $d(P_{M,N})$.

D. Algorithm Applicability, Advantages, and Limitations

In practice, the M_P and N_P are limited, and Δf is generally a small value, thus Δu is also limited. StepClimb in mono-valley and bi-valley cases can be sufficient to cover all the cases for the SDP solution in LEO constellation networks. Also, although StepClimb is derived based on the precondition that SDP is within the MHP set, the application of the algorithm is not limited to the precondition. The simulation results in the next section show that StepClimb can achieve high accuracy in generic scenarios.

Since the satellites in LEO constellation are dense and the SDP issue becomes more critical, this paper focuses on LEO constellations. But the application of the proposed algorithm is not limited to LEO space. When the satellite altitude can exceed the range of LEO, the algorithm still works as long as the constellation adopts a Walker pattern and the predefined four-ISL pattern. In a LEO mega-constellation with multiple shells, the algorithm is applicable to each shell, but not suitable for the case with cross-layer links. Also, the satellite can establish inter-plane ISL with farther neighbors on the non-adjacent plane. The calculation of $\Delta\Omega$ and Δf should be modified accordingly, and Δu can be larger. The algorithm still works in the mono-valley and bi-valley cases. Note that all the satellites should adopt the same ISL connection rule. Besides, StepClimb focuses on the SDP between two satellites. When evaluating the SDP between two ground stations, once the access satellites are determined, then ground-satellite link distances, u_0, M, and N are known, StepClimb can solve the end-to-end SDP between two ground stations.

Moreover, consider a special case when $\Delta f = 0$, then $T_i = U^s$ for $i = 1, 2, \ldots, N-1$, the problem is greatly simplified. The result is that all the inter-plane hops in SDP are successively taken at the phase where the inter-plane ISLs are shortest, which matches the popular SDP scheme in which all the inter-plane hops are successively taken at the higher latitudes [26], [27], [35].

In addition to the intuitiveness in theory, the advantage of StepClimb is the reduced computational complexity. Those graph-based algorithms depend on the topology information of the whole involved graph and iterative relaxation calculation. The computational complexity of Dijkstra and Bellman-Ford algorithm for the single-source shortest-path problem is $O(N_S^2)$ and $O(N_S N_L)$ [8], respectively, where N_S and N_L are the total satellite number and total edge number. Also, their complexity increases non-linearly with the constellation scale. However, once the constellation parameter and satellite phases are given, StepClimb can directly solve the SDP without graph construction or iterative calculation. The proposed explicit analytic algorithm can achieve $O(1)$, which greatly reduces computational complexity and is more significant in emerging mega-constellations. With a lower complexity and less required input, StepClimb could be potentially integrated into a distributed routing strategy. In the following section, the time consumption will be compared in the simulations.

The limitation of StepClimb is that it depends on a regular constellation topology. In practice, the non-uniform satellite phase distribution or node/link failure may cause an irregular topology and lead to minor deviations in the SDP. But the proposed StepClimb is still applicable because the basic topology features remain valid. The effects of the irregular topology are evaluated in the next section which shows that the errors are also acceptable.

V. Simulation Verification and Discussions

Through numerical simulations in various LEO constellation scenarios, this section first verifies the derived propositions and StepClimb in mono-valley case, then verifies the accuracy of StepClimb in bi-valley case and investigates the deviations. Finally, the SDP characteristics in Starlink constellation are further analyzed.

A. Simulation Settings

The Monte-Carlo method is adopted to verify the proposed propositions and algorithm. We randomly generate 1×10^6 LEO constellation scenarios with uniformly distributed random α, M_P, N_P, and F. In each scenario, the simulations iterate through paths with all the available M and N and u_0. The value ranges are listed in Table II.

The simulations are implemented on a computer with an Intel Core i5-1135G7 CPU @2.4 GHz and 16 GB RAM. The simulations involves orbit propagation, graph-topology construction, SDP calculation and result analysis. In a scenario case, once the constellation parameters and the phase of source satellite are given, all the satellite phases and ISL distances can be calculated, and the graph topology is established. Then a comparative algorithm, e.g., Dijkstra or LSP, is adopted to solve the SDP in the global topology. The constellation motion is featured by the varying satellite phases. Note that The solution of StepClimb only involves direct numerical calculations, while the orbit propagation, ISL distance or graph-related calculations are not required.

TABLE II

Variable Ranges of the Monte-Carlo Simulations

Variable	Range	Variable type
α	[40,70] deg	Continuous random variable
M_P	$\{4, 5, \ldots, 50\}$	Integer random variable
N_P	$\{4, 5, \ldots, 50\}$	Integer random variable
F	$\{0, 1, \ldots, N_P - 1\}$	Integer random variable
M	$\{2, 3, \ldots, \left\lfloor \frac{M_P}{2} \right\rfloor\}$	Integer ergodic variable
N	$\{2, 3, \ldots, \left\lfloor \frac{N_P}{2} \right\rfloor\}$	Integer ergodic variable
u_0	$\left[-\frac{\Delta f}{2}, 2\pi - \frac{\Delta f}{2}\right]$	Continuous ergodic variable with step 0.01

B. Verification in Mono-Valley Case

1) Verification of Propositions: We first verify Proposition 3 and 4, i.e., if all the inter-plane hops are successively taken and if all the SDPs have the minimum total phase offset. In the mono-valley case, u_0 is limited by $u_0 \in \left[-\frac{\Delta f}{2}, \pi - \frac{\Delta f}{2} - \Delta u\right]$. The SDP is solved using the traditional Dijkstra method. We examine each SDP and find that in all the SDPs the inter-plane hops are successively taken and all the SDPs have the minimum total phase offset, which can verify Proposition 3 and 4.

2) Verification of StepClimb *Solution:* We also adopted the Monte-Carlo method to verify the SDP solution of StepClimb in mono-valley cases, using the same scenario settings as in Table II. We generate 1×10^6 scenarios, and in each scenario, all the available M, N, and u_0 are tested. All the SDP distances of StepClimb are identical to the results of Dijkstra algorithm in the global topology, which verifies StepClimb.

In some special cases, although the SDPs of StepClimb and Dijkstra algorithms are different, they have the same distance. In these cases, we find that the SDPs are not unique. The inter-plane hops in these SDPs can happen at either v_1 or $v_1 + 1$, the total phase offsets are the same, and the path distances are the same minimum. According to (16) and (17), when solving v_1 and the value in the round function is exactly $K + 0.5$, where K is an integer, then either $v_1 = K$ or $K + 1$ would lead to the same phase offset, which explains the non-unique SDPs and also matches Proposition 4.

The time consumption of different SDP algorithms is also compared with other accurate benchmark algorithms. The Celestri (7×9), Iridium (6×11), Oneweb (18×36), Kuiper (34×34), Starlink-a (72×22) and Starlink-b (24×66) (see detailed parameters in [16]) are adopted as the constellation, respectively, where $N_P \times M_p$ indicates the constellation scale. In each constellation scenario, we generate 1×10^6 source-destination pairs with random M, N, and u_0 to solve the SDP using Dijkstra, DAG, and StepClimb, respectively. The time consumption is compared in Table III.

Table III shows that StepClimb can effectively reduce time consumption. The saved time can be over 99.4% and 74.0% compared to Dijkstra and DAG, respectively. The results in Table III also show that the time-saving ratio increases with the constellation scale, which indicates that the proposed

TABLE III
TIME CONSUMPTION COMPARISON OF DIFFERENT SDP ALGORITHMS

Constellation scale $N_P \times M_p$	7×9	6×11	18×36	34×34	72×22	24×66
Dijkstra	93.1 s	95.9 s	351.0 s	615.6 s	1771.4 s	1785.6 s
DAG	8.1 s	8.3 s	17.0 s	19.1 s	26.9 s	36.5 s
STEPCLIMB	5.0 s	5.1 s	7.2 s	7.1 s	9.5 s	9.6 s

STEPCLIMB has more remarkable advantages in large-scale constellations, e.g., Starlink. The reason is that in large-scale constellations, M and N are larger, and the traditional recursive algorithm would consume more time than the explicit analytic algorithm.

C. Verification in Bi-Valley Case

A similar Monte-Carlo simulation method and scenario settings are adopted to verify STEPCLIMB in the bi-valley case. We randomly generate 1×10^6 scenarios, and in each scenario all the available M, N, and u_0 are sampled. In the bi-valley case, u_0 is specified by $u_0 \in \left[-\frac{\Delta f}{2}, \pi - \frac{\Delta f}{2} - \Delta u\right]$ when $0 < \Delta u < \pi$, and $u_0 \in \left[-\frac{\Delta f}{2}, 2\pi - \frac{\Delta f}{2} - \Delta u\right]$ when $\pi \leq \Delta u < 2\pi$. Since STEPCLIMB in the bi-valley case is not strictly proved and the SDP solution is approximate, some errors may occur compared to the Dijkstra solution in global topology. The Mean Relative Error (MRE) is adopted to evaluate the relative error which is defined as follows,

$$\text{MRE} = \frac{1}{N_{\text{path}}} \sum_{i=1}^{N_{\text{path}}} \left| \frac{\hat{d}_i - d_i}{d_i} \right| \tag{26}$$

where N_{path} is the total path samples tested, d_i and $\hat{d}_i$ are the shortest path distances obtained by Dijkstra and STEPCLIMB, respectively. The maximum value of the relative errors (Max. RE) is also calculated. Moreover, we calculate the ratio of the path cases that the SDP solution is identical to the Dijkstra algorithm, which is taken as the Optimal SDP Probability.

To compare the errors, we also adopt three similar approximate algorithms, i.e., RandMHP, LSP [25], and DisCoRoute [26]. To reduce computations, all these algorithms limit their SDP discovery space to the MHP subgraph. RandMHP randomly decides the next hop direction at each node in the corresponding MHP region. It is a probabilistic routing and its results can be taken as a benchmark reference [26]. In LSP algorithm, the path always selects the direction with more remaining hops towards the destination, which can save distance by avoiding successive longer inter-plane ISLs. In DisCoRoute, satellites are iterated from the source and destination, respectively, and the successive satellites with minimum latitudes are selected to take the inter-plane hops. DisCoRoute aims to distribute the inter-plane hops to the high-latitude area where the inter-plane ISLs are shorter.

The errors in bi-valley cases are compared in Table IV. The average relative error of STEPCLIMB is only 0.11%, and the maximum error is as low as 7.18%. Over 77% of the obtained paths have an identical distance as the optimal solution. If the mono-valley case is also included, STEPCLIMB

TABLE IV
PERFORMANCE OF STEPCLIMB IN BI-VALLEY CASES

	RandMHP	LSP	DisCoRoute	STEPCLIMB	STEPCLIMB (overall)
MRE	8.82 %	8.16 %	1.1 %	0.11 %	0.09 %
Max. RE	151.39 %	145.18 %	97.31 %	7.18 %	7.32 %
Opt. SDP Prob.	9.67 %	23.86 %	41.88 %	77.75 %	83.38 %

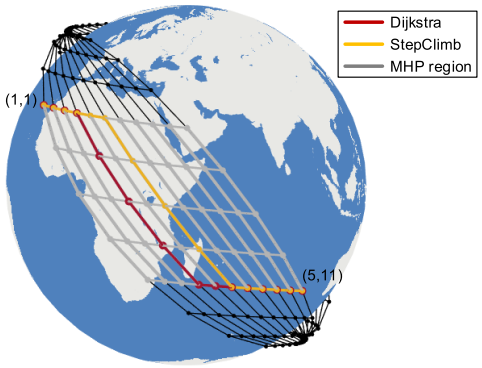

Fig. 9. An example of the path solution difference between Dijkstra and STEPCLIMB in the Starlink scenario.

TABLE V
ERRORS OF STEPCLIMB IN VARIOUS CONSTELLATION SCALES

Constellation scale $N_P \times M_p$	Celestri 7x9	Iridium 6x11	Oneweb 18x36	Kuiper 34x34	Starlink-a 72x22	Starlink-b 24x66
MRE	0	0.10%	0.04%	0.01%	0.01%	0.002%
Max. RE	0	2.84%	2.13%	0.41%	0.62%	0.25%
Opt. SDP Prob.	100%	90.42%	86.31%	91.16%	86.23%	95.01%

(overall) results show the overall STEPCLIMB performance in all cases is further improved. The overall relative error is lower than 0.1%. Compared to the RandMHP and LSP algorithm, the solution accuracy is much higher, which indicates the proposed STEPCLIMB is applicable and effective in both mono-valley and bi-valley cases. Also, the error is much less than DisCoRoute, because DisCoRoute is not strictly derived and the higher satellite latitude cannot strictly guarantee the absolute shortest path.

To further investigate the path deviation, Fig. 9 illustrates an example of the path solution difference in the Starlink Scenario with $M = 5$, $N = 11$. Although error exists, the two paths are much close, and the relative error in path distance is only 0.02%. The reason is that the solution of R in STEPCLIMB is not accurate, thus the obtained path may have different successive inter-plane hops. We can also find that all the inter-plane hops occur at the high altitudes within the MHP region where the inter-plane ISLs are shorter.

The errors of STEPCLIMB in bi-valley cases are also evaluated in various constellation scales. The scenario settings are the same with mono-valley cases in Table II. The results are shown in Table V and Fig. 10. The error decreases with the constellation scale, which indicates STEPCLIMB has better performance in mega-constellation constellations. In Starlink scenario, the MRE can be lower than 0.01%. The reason is that the ISL distances are shorter in mega-constellations, and the path distance difference caused by the path deviation can

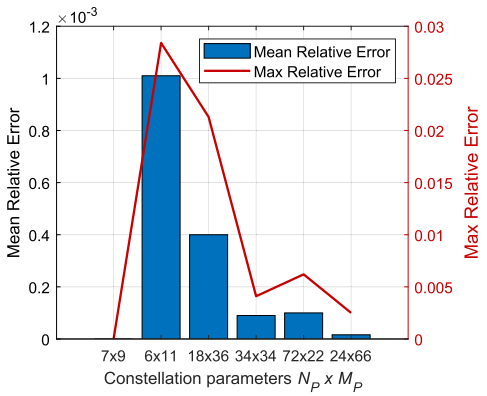

Fig. 10. Errors of StepClimb in various constellation scales.

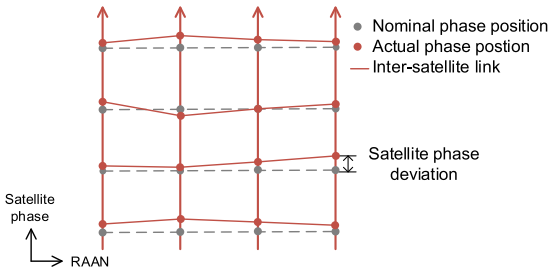

Fig. 11. Non-uniform satellite phase position in actual constellations.

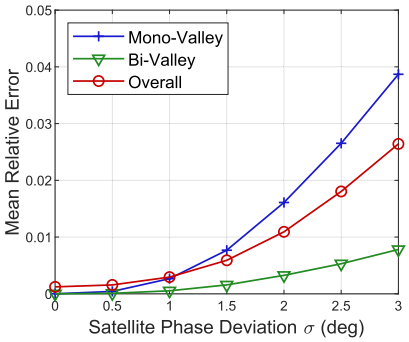

Fig. 12. StepClimb error in Starlink 72×22 constellation with non-uniform satellite phase placement.

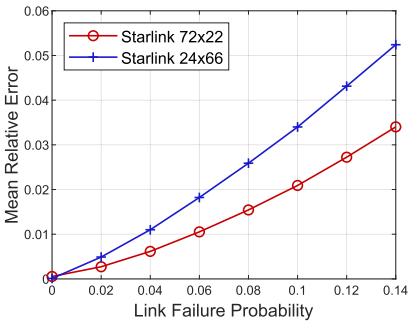

Fig. 13. StepClimb error in Starlink constellation with random link failures.

be reduced. Also, we can find that in some special scenarios, e.g., Celestri constellation, StepClimb achieves zero error.

D. Performance Evaluation in Irregular Topology

As discussed in Section IV-D, StepClimb requires a regular constellation topology. Here we study the algorithm error in irregular topologies, considering the non-uniform satellite placement and link failures.

First, Fig. 11 shows the non-uniform satellite placement in real constellations. Due to the orbit perturbation, the satellite phases may have deviations compared to their nominal position [36], [37]. Then we add a random deviation δu to the nominal phase of each satellite to simulate the actual satellite phase, where $\delta u \sim \mathcal{N}(0, \sigma^2)$. Fig. 12 indicates that StepClimb error increases with the phase deviations in Starlink 72×22 constellation case. The relative error in mono-valley cases is greater than in bi-valley cases, because the paths in bi-valley cases may have more intra-plane ISLs which are successive, and the impacts of the non-uniform satellite phase of successive inter-plane ISL are offset. The absolute errors are close but bi-valley path distances are longer. It also indicates that when the end satellites are far away, the effects of non-uniform phase distribution become weaker. Since the satellite phase can be maintained by the thruster, when the phase deviations are maintained within 1 deg, StepClimb error can be smaller than 0.3%. According to the literature [36], the phase deviation in Starlink maintains within only 0.2 deg in most time and peaks at 0.5 deg, which means the proposed algorithm is applicable in practice.

When link failures are considered, performance of StepClimb is further evaluated. The link failure occurs randomly on each link with equal probability. Fig. 13 shows that the SDP distance error of StepClimb increases with the link failure probability, because the links in the ideal SDP can be unavailable and a detour happens. In the Starlink scenario with 1584 satellites, the mean error can be lower than 4% when the link failure probability is within 0.1. In different constellation configurations, StepClimb performs better in the 72×22 configuration than the 24×66 case. The reason is that the error is only caused by the inter-plane ISLs, and 72×22 configuration has more orbits and shorter inter-plane ISLs. When an inter-plane ISL is unavailable, the affected path segment can be smaller when the ISLs are shorter. When 5% links become unavailable in Starlink 72×22 constellation, the mean error is only 0.83%.

E. Analysis of SDP in Mega-Constellations

This section further investigates the SDP characteristics in mega-constellations. According to the above SDP solution model, in a given constellation, the SDP is determined by M, N and u_0. First u_0 is studied with fixed M and N. Based on the Starlink 72×22 constellation, Fig. 14 illustrates the SDP distance variation during the satellite movement. When M, N are fixed, the SDP distance between two satellite nodes varies with the u_0. Note that in these cases, Δu is within 35∼52 deg range. When the source satellite is around u_0=160 deg, all the involved satellites between (1,1) and (M, N) are over the low-latitude regions, where the inter-plane ISLs are longer, thus the SDP distance also achieves the maximum. The relative variation range at the peak is 9.26% in the case of $(M = 3, N = 5)$. Since the variation of the SDP distance is caused by the inter-plane ISLs, when the inter-plane hops increase, the relative variation also increases. For example, when N increases from 5 to 6, the relative variation range at the peak

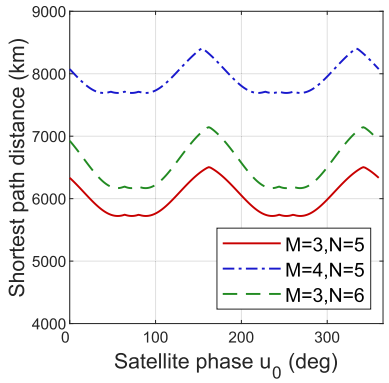

Fig. 14. SDP distance variation with satellite movement. The source and destination nodes are fixed at (1,1) and (M, N) in Starlink scenario.

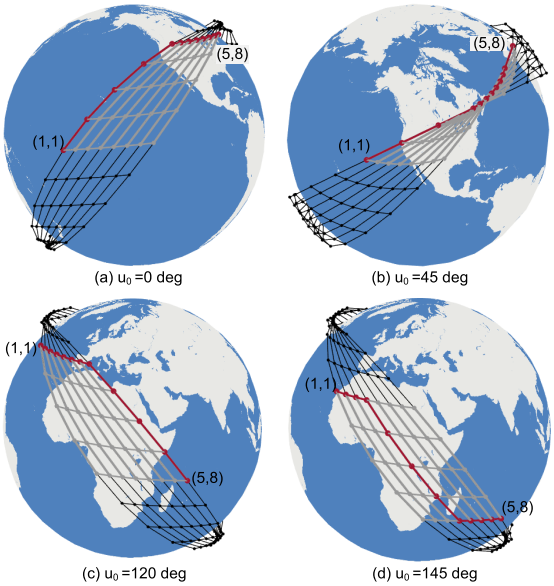

Fig. 15. SDP pattern variation with different satellite phases in Starlink when satellites are moving. The gray lines indicate the corresponding MHP region.

is up to 15.80%. Therefore, a path with more inter-plane hops may have a greater variation during the satellite movement.

During the satellite movement, the pattern of SDP between two satellites also changes. Fig. 15 demonstrates the SDP pattern variation between (1,1) and (5, 8) in Starlink scenario. It can be found that all the SDPs are within the MHP region, and most of the inter-plane hops occur successively. But the SDPs have different shapes when the satellites move. When u_0=45 deg, the SDP is the shortest, where all the inter-plane hops happen in the polar regions and the inter-plane ISLs are shortest. When u_0=145 deg, the inter-plane hops are separated into two parts and each part is at the highest latitude. The underlying cause is that the inter-plane hops tend to happen at higher latitudes where the inter-plane ISLs are shorter. This also indicates that when the shortest path rule is always adopted, the SDP-involved satellites will be changing, and satellites in the high latitude regions may carry more traffic.

VI. Conclusion

To solve the SDP in LEO constellation networks, different from those widely applied graph-based iterative algorithms, this paper focuses on an explicit analytic approach. By exploiting the topological regularity and ISL distance features, the SDP problem can be deduced into a minimum path offset problem. Through derivations, StepClimb is proposed. The proposed algorithm can greatly reduce the computational cost with high accuracy compared to traditional algorithms. The derivations prove that most inter-plane hops in the SDP occur successively, and the simulations further indicate that these hops prefer satellites in the higher latitude regions. This work has significance in LEO constellation network routing issues in both theory and practice.

Appendix A
Proof of Proposition 1

Proof: Since $\Delta u \in \left[0, \frac{\pi}{2} - \widetilde{u_0}\right]$, the nearest symmetry axis of all the involved nodes is the same one $u = U^s$. Then $\sum_{i=1}^{N-1} |\widetilde{u}(v_i)| = \sum_{i=1}^{N-1} |u(v_i) - U^s|$, where $U^s = k_1\pi + \frac{\pi}{2} - \frac{\Delta f}{2}$ and $k_1 = \left\lfloor \frac{u_0 + \Delta f/2}{\pi} \right\rfloor$. $\sum_{i=1}^{N-1} |\widetilde{u}(v_i)| = |u(v_1) - U^s| + |u(v_1) + (v_2 - v_1)\Delta\Phi + \Delta f - U^s| + |u(v_1) + (v_3 - v_1)\Delta\Phi + 2\Delta f - U^s| + \ldots + |u(v_1) + (v_{N-1} - v_1)\Delta\Phi + (N-2)\Delta f - U^s|$. The above formula means the sum of the distance between $u(v_1)$ and $N-1$ points on the real axis, i.e., U^s, $U^s - (v_2 - v_1)\Delta\Phi - \Delta f$, $\ldots$, $U^s - (v_{N-1} - v_1)\Delta\Phi - (N-2)\Delta f$.

Due to $v_i \le v_{i+1}$ and $v_i \in \{1, 2, \ldots, M\}$, the above $N-1$ points are progressively decreased. To achieve the minimum sum of the distances, the $N-1$ points should be as close as possible, thus $v_1 = v_2 = \ldots = v_{N-1}$. □

Appendix B
Proof of Proposition 2

Proof: According to (14) and Fig. 6, $\sum_{i=1}^{N-1} |\widetilde{u}(v_i)|$ means the sum of the distance between $u(v_1)$ and $N-1$ points on the real axis, i.e., U^s, $U^s - \Delta f$, $U^s - 2\Delta f$,..., $U^s - (N-2)\Delta f$. Then the optimal value of $u(v_1)$, or v_1, depends on if $N-1$ is even or odd.

1) If $N-1$ is even, to ensure (14) to be minimum, $u(v_1)$ should be between $U^s - \left(\frac{N-1}{2} - 1\right)\Delta f$ and $U^s - \frac{N-1}{2}\Delta f$. Since $u(v_1)$ is discrete, $u(v_1)$ should be closest to the mid-point of the two points, i.e., $U^s - \frac{N-2}{2}\Delta f$. Then $v_1 = \arg\min_{v_1} \left|u(v_1) + \frac{N-2}{2}\Delta f - U^s\right|$.

2) If $N-1$ is odd, to ensure (14) to be minimum, $u(v_1)$ should be closest to the middle points of the $N-1$ points, i.e., $U^s - \frac{N-2}{2}\Delta f$. Also, we can obtain $v_1 = \arg\min_{v_1} \left|u(v_1) + \frac{N-2}{2}\Delta f - U^s\right|$. □

Appendix C
Proof of Proposition 3

Proof: Proof by contradiction is adopted. First, assume $\min_{v_i} \sum_{i=1}^{N-1} d^H(u(v_i))$ is achieved in a given path with $v_{L+1} - v_L = \Delta v > 0$, where $L \in \{1, 2, N-2\}$. We have $u(v_{L+1}) = u(v_L) + \Delta v\Delta\Phi + \Delta f$. We divide the proof into two cases based on whether $2u(v_L) + \Delta v\Delta\Phi < 2U^s$.

(1) If $2u(v_L) + \Delta v\Delta\Phi < 2U^s$, then $U^s - u(v_L) > u(v_L) + \Delta v\Delta\Phi - U^s$. Also, $U^s - u(v_L) > U^s - u(v_L) -$

$\Delta v\Delta\Phi$, thus $|U^s - u(v_L)| > |U^s - u(v_L) - \Delta v\Delta\Phi| = |U^s - u(v_L + \Delta v)|$, $d^H(u(v_L)) > d^H(u(v_L + \Delta v))$. For the given shortest path, if $v'_L = v_L + \Delta v$, then the generated new path is feasible and has a shorter distance.

(2) If $2u(v_L) + \Delta v\Delta\Phi \geq 2U^s$, then $2u(v_L) + \Delta v\Delta\Phi + 2\Delta f > 2U^s$, $u(v_L) + \Delta v\Delta\Phi + \Delta f - U^s > U^s - u(v_L) - \Delta f$, $u(v_{L+1}) - U^s > U^s - u(v_{L+1}) + \Delta v\Delta\Phi$. Also, $u(v_{L+1}) - U^s > u(v_{L+1}) - \Delta v\Delta\Phi - U^s$, thus $|u(v_{L+1}) - U^s| > |u(v_{L+1}) - \Delta v\Delta\Phi - U^s| = |u(v_{L+1} - \Delta v) - U^s|$, $d^H(u(v_{L+1})) > d^H(u(v_{L+1} - \Delta v))$. For the given shortest path, if $v'_{L+1} = v_{L+1} - \Delta v$, then the generated new path is feasible and has a shorter distance.

Combining the above two cases, the assumption does not hold, then for $i = 1, 2, N-2$, $v_{i+1} - v_i = 0$, i.e., $v_1 = v_2 = \ldots = v_{N-1}$. □

APPENDIX D
PROOF OF PROPOSITION 4

Proof: First we expand the available value range of $u(v_1)$ to be continuous, $u(v_1) \in [u_0, u_0 + (M-1)\Delta\Phi]$. According to Proposition 2, when $\sum_{i=1}^{N-1} |\widetilde{u}(v_i)|$ is minimized, $\left|\frac{u(v_1)+u(v_{N-1})}{2} - U^s\right|$ is also minimized. Proposition 2 and 3 further indicate that in the SDP, $v_1 = v_2 = \ldots = v_{N-1}$. Assume another MHP where the i-th inter-plane hop occurs at $u'(v_i)$. Let $u'(v_i) = u(v_i) + \delta$ and $\tilde{u}'(v_i) = |u'(v_i) - U^s|$

(1) If $\frac{u(v_1)+u(v_{N-1})}{2} - U^s = 0$ and $\delta > 0$, we have $\tilde{u}'(v_1) < \tilde{u}(v_1) = \tilde{u}(v_{N-1}) < \tilde{u}'(v_{N-1})$, $\tilde{u}'(v_1) = \tilde{u}(v_1) - \delta$, and $\tilde{u}'(v_{N-1}) = \tilde{u}(v_{N-1}) + \delta$. According to the monotonicity of $\frac{\mathrm{d}d^H(u)}{\mathrm{d}u}$ and the definition of $d^H(\tilde{u})$, we have $\frac{\mathrm{d}^2 d^H(\tilde{u})}{\mathrm{d}\tilde{u}^2} > 0$. Based on the Lagrangian middle-value theorem, $d^H(\tilde{u}(v_1)) + d^H(\tilde{u}(v_{N-1})) < d^H(\tilde{u}'(v_{N-1})) + d^H(\tilde{u}'(v_1))$. Similarly, we have $d^H(\tilde{u}(v_2)) + d^H(\tilde{u}(v_{N-2})) < d^H(\tilde{u}'(v_{N-2})) + d^H(\tilde{u}'(v_2))$, $\cdots$ Finally, $\sum_{i=1}^{N-1} d^H(u(v_i)) < \sum_{i=1}^{N-1} d^H(u'(v_i))$.

If $\delta < 0$, then $\tilde{u}'(v_{N-1}) < \tilde{u}(v_1) = \tilde{u}(v_{N-1}) < \tilde{u}'(v_1)$. Also, $\sum_{i=1}^{N-1} d^H(u(v_i)) < \sum_{i=1}^{N-1} d^H(u'(v_i))$.

(2) If $\frac{u(v_1)+u(v_{N-1})}{2} - U^s > 0$, then $u(v_1) > U^s$, or we can find $L \in \left\{1, 2, \lfloor\frac{N-1}{2}\rfloor\right\}$ so that $u_L < U^s$ and $u_{L+1} > U^s$. Let $u'(v_i) = u(v_i) + \delta$. Since $\left|\frac{u(v_1)+u(v_{N-1})}{2} - U^s\right|$ has been minimized, δ should be $\delta > 0$. Then $\tilde{u}'(v_1) < \tilde{u}(v_1) < \tilde{u}(v_{N-1}) < \tilde{u}'(v_{N-1})$. Based on the Lagrangian middle-value theorem, $d^H(\tilde{u}(v_1)) + d^H(\tilde{u}(v_{N-1})) < d^H(\tilde{u}'(v_{N-1})) + d^H(\tilde{u}'(v_1))$, $d^H(\tilde{u}(v_2)) + d^H(\tilde{u}(v_{N-2})) < d^H(\tilde{u}'(v_{N-2})) + d^H(\tilde{u}'(v_2))$, $\ldots$, $d^H(\tilde{u}(v_L)) + d^H(\tilde{u}(v_{N-L})) < d^H(\tilde{u}'(v_{N-L})) + d^H(\tilde{u}'(v_L))$. Also, $d^H(\tilde{u}(v_{L+1})) < d^H(\tilde{u}'(v_{L+1}))$, $\ldots$, $d^H(\tilde{u}(v_{N-L-1})) < d^H(\tilde{u}'(v_{N-L-1}))$. Then $\sum_{i=1}^{N-1} d^H(u(v_i)) < \sum_{i=1}^{N-1} d^H(u'(v_i))$.

(3) Similarly, if $\frac{u(v_1)+u(v_{N-1})}{2} - U^s < 0$, we can also obtain $\sum_{i=1}^{N-1} d^H(u(v_i)) < \sum_{i=1}^{N-1} d^H(u'(v_i))$.

The above formulations indicate that when $\left|\frac{u(v_1)+u(v_{N-1})}{2} - U^s\right|$ is minimized, i.e., $v_1 = \arg\min_{v_1} \left|u(v_1) + \frac{N-2}{2}\Delta f - U^s\right|$, $u(v_1) + \delta$ will result in a larger $\sum_{i=1}^{N-1} d^H(u(v_i))$. In the discrete case, $\delta = k\Delta\Phi$, the conclusion is also applicable. Therefore, when $\sum_{i=1}^{N-1} |\widetilde{u}(v_i)|$ is minimized, $\min_{v_i} \sum_{i=1}^{N-1} d^H(u(v_i))$ is also achieved. □

REFERENCES

[1] M. Handley, "Delay is not an option," in *Proc. 17th ACM Workshop Hot Topics Netw.*, Nov. 2018, pp. 85–91.

[2] W. Xia, C. Di, H. Guo, and S. Li, "Reinforcement learning based stochastic shortest path finding in wireless sensor networks," *IEEE Access*, vol. 7, pp. 157807–157817, 2019.

[3] Y. Lu et al., "Enhancing transmission efficiency of mega-constellation LEO satellite networks," *IEEE Trans. Veh. Technol.*, vol. 71, no. 12, pp. 13210–13225, Dec. 2022.

[4] H. Zhu, Q. Chen, X. Zhu, W. Yao, and X. Chen, "Edge computing powers aerial swarms in sensing, communication, and planning," *Innovation*, vol. 4, no. 6, Nov. 2023, Art. no. 100506.

[5] A. U. Chaudhry and H. Yanikomeroglu, "When to crossover from earth to space for lower latency data communications?" *IEEE Trans. Aerosp. Electron. Syst.*, vol. 58, no. 5, pp. 3962–3978, Oct. 2022.

[6] Z. Lin et al., "Systematic utilization analysis of mega-constellation networks," in *Proc. Int. Wireless Commun. Mobile Comput.*, 2022, pp. 1317–1322.

[7] X. Qin, T. Ma, Z. Tang, X. Zhang, H. Zhou, and L. Zhao, "Service-aware resource orchestration in ultra-dense LEO satellite–terrestrial integrated 6G: A service function chain approach," *IEEE Trans. Wireless Commun.*, vol. 22, no. 9, pp. 6003–6017, 2023, doi: 10.1109/TWC.2023.3239080.

[8] W. Peng, X. Hu, F. Zhao, and J. Su, "A fast algorithm to find all-pairs shortest paths in complex networks," *Proc. Comput. Sci.*, vol. 9, pp. 557–566, Jan. 2012.

[9] R. De Gaudenzi, M. Luise, and L. Sanguinetti, "The open challenge of integrating satellites into (beyond-) 5G cellular networks," *IEEE Netw.*, vol. 36, no. 2, pp. 168–174, Mar. 2022.

[10] D. Zhou, M. Sheng, J. Li, and Z. Han, "Aerospace integrated networks innovation for empowering 6G: A survey and future challenges," *IEEE Commun. Surveys Tuts.*, vol. 25, no. 2, pp. 975–1019, 2nd Quart., 2023.

[11] X. Deng, L. Chang, S. Zeng, L. Cai, and J. Pan, "Distance-based back-pressure routing for load-balancing LEO satellite networks," *IEEE Trans. Veh. Technol.*, vol. 72, no. 1, pp. 1240–1253, Jan. 2023.

[12] Z. Lai, H. Li, and J. Li, "STARPERF: Characterizing network performance for emerging mega-constellations," in *Proc. Int. Conf. Netw. Protocols*, 2020, pp. 1–11.

[13] T. Ma, B. Qian, X. Qin, X. Liu, H. Zhou, and L. Zhao, "Satellite-terrestrial integrated 6G: An ultra-dense LEO networking management architecture," *IEEE Wireless Commun.*, early access, Dec. 12, 2022.

[14] S. Zhang and K. L. Yeung, "Scalable routing in low-earth orbit satellite constellations: Architecture and algorithms," *Comput. Commun.*, vol. 188, pp. 26–38, Apr. 2022.

[15] Y. Huang et al., "Reinforcement learning based dynamic distributed routing scheme for mega LEO satellite networks," *Chin. J. Aeronaut.*, vol. 36, no. 2, pp. 284–291, Feb. 2023.

[16] Q. Chen, G. Giambene, L. Yang, C. Fan, and X. Chen, "Analysis of inter-satellite link paths for LEO mega-constellation networks," *IEEE Trans. Veh. Technol.*, vol. 70, no. 3, pp. 2743–2755, Mar. 2021.

[17] T. Pan, T. Huang, X. Li, Y. Chen, W. Xue, and Y. Liu, "OPSPF: Orbit prediction shortest path first routing for resilient LEO satellite networks," in *Proc. IEEE Int. Conf. Commun. (ICC)*, May 2019, pp. 1–6.

[18] J. Li, H. Lu, K. Xue, and Y. Zhang, "Temporal netgrid model-based dynamic routing in large-scale small satellite networks," *IEEE Trans. Veh. Technol.*, vol. 68, no. 6, pp. 6009–6021, Jun. 2019.

[19] A. U. Chaudhry and H. Yanikomeroglu, "Laser intersatellite links in a starlink constellation: A classification and analysis," *IEEE Veh. Technol. Mag.*, vol. 16, no. 2, pp. 48–56, Apr. 2021.

[20] Q. Chen, L. Yang, D. Guo, B. Ren, J. Guo, and X. Chen, "LEO satellite networks: When do all shortest distance paths belong to minimum hop path set?" *IEEE Trans. Aerosp. Electron. Syst.*, vol. 58, no. 4, pp. 3730–3734, Aug. 2022.

[21] Z. Lai, W. Liu, Q. Wu, H. Li, J. Xu, and J. Wu, "SpaceRTC: Unleashing the low-latency potential of mega-constellations for real-time communications," in *Proc. IEEE Conf. Comput. Commun.*, May 2022, pp. 1339–1348.

[22] Q. Chen, L. Yang, G. Song, Z. Yin, H. Yang, and Y. Zhao, "Distance characteristics of paths with the minimum inter-satellite hops in LEO satellite networks," in *Proc. IEEE 22nd Int. Conf. Commun. Technol. (ICCT)*, Nov. 2022, pp. 458–462.

[23] S. Kassing, D. Bhattacherjee, A. B. Águas, J. E. Saethre, and A. Singla, "Exploring the 'internet from space' with hypatia," in *Proc. ACM Internet Meas. Conf.*, Oct. 2020, pp. 214–229.
[24] M. Hozayen, T. Darwish, G. K. Kurt, and H. Yanikomeroglu, "A graph-based customizable handover framework for LEO satellite networks," in *Proc. IEEE Globecom Workshops*, Dec. 2022, pp. 868–873.
[25] Q. Chen, X. Chen, L. Yang, S. Wu, and X. Tao, "A distributed congestion avoidance routing algorithm in mega-constellation network with multi-gateway," *Acta Astronautica*, vol. 162, pp. 376–387, Sep. 2019.
[26] G. Stock, J. A. Fraire, and H. Hermanns, "Distributed on-demand routing for LEO mega-constellations: A starlink case study," in *Proc. 11th Adv. Satell. Multimedia Syst. Conf. 17th Signal Process. Space Commun. Workshop (ASMS/SPSC)*, Sep. 2022, pp. 1–8.
[27] E. Ekici, I. F. Akyildiz, and M. D. Bender, "A distributed routing algorithm for datagram traffic in LEO satellite networks," *IEEE/ACM Trans. Netw.*, vol. 9, no. 2, pp. 137–147, Apr. 2001.
[28] A. U. Chaudhry and H. Yanikomeroglu, "Temporary laser inter-satellite links in free-space optical satellite networks," *IEEE Open J. Commun. Soc.*, vol. 3, pp. 1413–1427, 2022.
[29] A. U. Chaudhry, G. Lamontagne, and H. Yanikomeroglu, "Laser inter-satellite link range in free-space optical satellite networks: Impact on latency," *IEEE Aerosp. Electron. Syst. Mag.*, vol. 38, no. 4, pp. 4–13, Apr. 2023.
[30] A. U. Chaudhry and H. Yanikomeroglu, "Optical wireless satellite networks versus optical fiber terrestrial networks: The latency perspective," in *Proc. 30th Biennial Symp. Commun.*, Cham, Switzerland, 2021, pp. 225–234.
[31] J. Guo, L. Yang, D. Rincón, S. Sallent, Q. Chen, and X. Liu, "Static placement and dynamic assignment of SDN controllers in LEO satellite networks," *IEEE Trans. Netw. Service Manag.*, vol. 19, no. 4, pp. 4975–4988, Dec. 2022.
[32] Q. Chen, L. Yang, J. Guo, X. Liu, and X. Chen, "Optimal gateway placement for minimizing intersatellite link usage in LEO megaconstellation networks," *IEEE Internet Things J.*, vol. 9, no. 22, pp. 22682–22694, Nov. 2022.
[33] W. Wang, Y. Zhao, Y. Zhang, X. He, Y. Liu, and J. Zhang, "Intersatellite laser link planning for reliable topology design in optical satellite networks: A networking perspective," *IEEE Trans. Netw. Service Manag.*, vol. 19, no. 3, pp. 2612–2624, Sep. 2022.
[34] O. Kodheli et al., "Satellite communications in the new space era: A survey and future challenges," *IEEE Commun. Surveys Tuts.*, vol. 23, no. 1, pp. 70–109, 1st Quart., 2021.
[35] Q. Chen, L. Yang, X. Liu, B. Cheng, J. Guo, and X. Li, "Modeling and analysis of inter-satellite link in LEO satellite networks," in *Proc. 13th Int. Conf. Commun. Softw. Netw. (ICCSN)*, Jun. 2021, pp. 134–138.
[36] Y. Sun and H. Shen, "The control of mega-constellation at low earth orbit based on TLE," *Mech. Eng.*, vol. 42, no. 2, pp. 156–162, 2020.
[37] N. Reiland, A. J. Rosengren, R. Malhotra, and C. Bombardelli, "Assessing and minimizing collisions in satellite mega-constellations," *Adv. Space Res.*, vol. 67, no. 11, pp. 3755–3774, Jun. 2021.

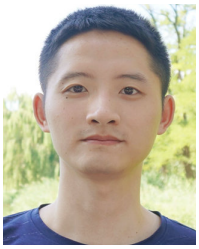

Quan Chen received the B.E. and Ph.D. degrees from the National University of Defense Technology (NUDT), Changsha, China, in 2015 and 2021, respectively. He is currently a Lecturer with the College of Aerospace Science and Engineering, NUDT. His research interests include mega-constellation satellite networks, UAV networks, and integrated space-terrestrial networks. He has served as an Associate Editor for *Telecommunication Systems* and a reviewer for several journals, including IEEE JOURNAL ON SELECTED AREAS IN COMMUNICATIONS, IEEE TRANSACTIONS ON WIRELESS COMMUNICATIONS, IEEE TRANSACTIONS ON MOBILE COMPUTING, IEEE TRANSACTIONS ON VEHICULAR TECHNOLOGY, and IEEE TRANSACTIONS ON AEROSPACE AND ELECTRONIC SYSTEMS. He has served as a TPC Member for IEEE ICC Workshop on Mega-Constellation from 2021 to 2023.

Lei Yang received the Ph.D. degree from the College of Aerospace Science and Engineering, National University of Defense Technology, Changsha, China, in 2008. His current research interests are focused on satellite communication networks, measurement and control technology for micro-satellite, on-board computer, spacecraft system modeling, and simulation. He is currently a member of the Chinese Society of Astronautics and China Instrument and Control Society.

Yong Zhao received the Ph.D. degree in aerospace science and engineering from the National University of Defense Technology, Changsha, China, in 2005. He is currently a Professor with the National University of Defense Technology. His research interests include micro/nano satellite design, spacecraft cluster application, and topological optimization.

Yi Wang received the Ph.D. degree in aerospace engineering from the National University of Defense Technology, Changsha, China, in 2019. His current research interests include spacecraft dynamics and control, aerospace engineering, and swarm intelligence.

Haibo Zhou (Senior Member, IEEE) received the Ph.D. degree from Shanghai Jiao Tong University in 2014. He is currently a Full Professor with the School of Electronic Science and Engineering, Nanjing University. He was a recipient of the 2019 IEEE ComSoc Asia–Pacific Outstanding Young Researcher Award, (2023–2024) IEEE ComSoc Distinguished Lecturer, and (2023–2025) IEEE VTS Distinguished Lecturer. His research interests include resource management and protocol design in B5G/6G networks, vehicular ad-hoc networks, and space-air-ground integrated networks.

Xiaoqian Chen received the M.S. and Ph.D. degrees in aerospace engineering from the National University of Defense Technology, China, in 1997 and 2001, respectively. He is currently a Professor with the Chinese Academy of Military Sciences and an Academician of the Chinese Academy of Sciences (CAS). His current research interests include spacecraft systems engineering, advanced digital design methods of space systems, and multidisciplinary design optimization.